J|A|C|S
ARTICLES
Published on Web 07/15/2006

Shape-Specific Detection Based on Fluorescence Resonance Energy Transfer Using a Flexible Water-Soluble Conjugated Polymer

Wei Lv,[†,§] Na Li,[†,§] Yuliang Li,[‡,§] Ye Li,[†,§] and Andong Xia*[,†,§]

State Key Laboratory of Molecular Reaction Dynamics, Institute of Chemistry, Chinese Academy of Sciences, Beijing-100080, P. R. China, The CAS Key Laboratory of Organic Solids, Institute of Chemistry, Chinese Academy of Sciences, Beijing-100080, P. R. China. and Beijing National Laboratory for Molecular Sciences (BNLMS), Institute of Chemistry, Chinese Academy of Sciences, Beijing-100080, P. R. China

Received April 30, 2006; E-mail: andong@iccas.ac.cn

Abstract: We present the detection of the shape-specific conformation of DNA based on the fluorescence resonance energy transfer (FRET) by using a novel flexible water-soluble cationic conjugated polymer (CCP). The flexible backbone of CCP has more conformational freedom with the potential to be responsive to analyte shape by electrostatic interaction between flexible CCP and negatively charged DNA. The analyte shape dependent recognition is accomplished by structural changes that compressed or extended the flexible CCP. The morphology-dependent spectral properties of the novel flexible polymer related to the analyte shapes are investigated in detail, where two types of chromophores, referred to as "isolated" segment and "packed" segment aggregates, within the flexible polymer are identified by means of ensemble and single molecule measurements upon binding with different geometric DNA. The change in fluorescence intensity upon binding with shape-specific DNA without obvious color shifts makes this novel flexible polymer a suitable CCP donor for FRET measurements. The results provide insights for understanding the spectral properties of flexible water-soluble CCP and CCP/DNA interaction related to the geometry of target analyte.

Introduction

Water-soluble cationic conjugated polymers (CCPs) have been strongly demonstrated to be good candidates as chem- or bio-sensors that exhibit rapid and collective responses to relatively small perturbations in local environments, especially for strand-specific bioploymer (such as DNA and RNA) detection based on their electrochemical and optical properties upon complexation with target biomolecules.[1−20] Among these protocols, fluorescence resonance energy transfer (FRET) is one of the tools widely used in biology to study biomolecular structures and dynamics, whereas the charged CCPs function as donors for light-harvesting, and the signaling fluorescent dyes labeled to the negatively charged biopolymers such as DNA and RNA function as acceptors.[6−12,21−24] Electrostatic interaction and hydrophobic interaction between flexible CCPs and phosphate groups in DNA and RNA could bring the dynamic structure of the CCP/DNA complexes, which may cause the complicated spectral behaviors of CCPs and FRET.[1−4,6,13,14,22,25]

Moreover, CCPs in previous studies frequently take the forms of rigid-rod structures, which have limited flexibility and limited spatial registry with the three-dimensional molecular shapes of

[†] State Key Laboratory of Molecular Reaction Dynamics.
[‡] The CAS Key Laboratory of Organic Solids.
[§] Beijing National Laboratory for Molecular Sciences (BNLMS).

(1) Gaylord, B. S.; Heeger, A. J.; Bazan, G. C. *Proc. Natl. Acad. Sci. U.S.A.* **2002**, *99*, 10954−10957.
(2) Leclerc, M. *Adv. Mater.* **1999**, *11*, 1491−1498.
(3) McQuade, D. T.; Pullen, A. E.; Swager, T. M. *Chem. Rev.* **2000**, *100*, 2537−2574.
(4) Chen, L.; McBranch, D. W.; Wang, H.; Helgeson, R.; Wudl, F.; Whitten, D. G. *Proc. Natl. Acad. Sci. U.S.A.* **1999**, *96*, 12287−12292.
(5) Gaylord, B. S.; Heeger, A. J.; Bazan, G. C. *J. Am. Chem. Soc.* **2003**, *125*, 896−900.
(6) Liu, B.; Bazan, G. C. *Chem. Mater.* **2004**, *16*, 4467−4476.
(7) Wang, D.; Gong, X.; Heeger, P. S.; Rininsland, F.; Bazan, G. C.; Heeger, A. J. *Proc. Natl. Acad. Sci. U.S.A.* **2002**, *99*, 49−53.
(8) Wang, S.; Gaylord, S. S.; Bazan, G. C. *J. Am. Chem. Soc.* **2004**, *126*, 5446−5451.
(9) Xu, Q. H.; Wang, S.; Korystov, D.; Mikhailovsky, A.; Bazan, G. C.; Moses, D.; Heeger, A. J. *Proc. Natl. Acad. Sci. U.S.A.* **2005**, *102*, 530−535.
(10) Wang, S.; Gaylord, B. S.; Bazan, G. C. *Adv. Mater.* **2004**, *16*, 2127−2132.
(11) Doré, K.; Dubus, S.; Ho, H. A.; Lévesque, I.; Brunette, M.; Corbeil, G.; Boissinot, M.; Boivin, G.; Bergeron, M. G.; Boudreau, D.; Leclerc, M. *J. Am. Chem. Soc.* **2004**, *126*, 4240−4244.
(12) Nilsson, K. P. R.; Inganäs, O. *Nat. Mater.* **2003**, *2*, 419−424.
(13) Dwight, S. J.; Gaylord, B. S.; Hong, J. W.; Bazan, G. C. *J. Am. Chem. Soc.* **2004**, *126*, 16850−16859.
(14) Liu, B.; Bazan, G. C. *J. Am. Chem. Soc.* **2006**, *128*, 1188−1196.
(15) Ho, H. A.; Boissinot, M.; Bergeron, M. G.; Corbeil, G.; Doré, K.; Boudreau, D.; Leclerc, M. *Angew. Chem., Int. Ed.* **2002**, *41*, 1548−1551.
(16) Ho, H. A.; Leclerc, M. *J. Am. Chem. Soc.* **2004**, *126*, 1384−1387.
(17) Liu, B.; Bazan, G. C. *J. Am. Chem. Soc.* **2004**, *126*, 1942−1943.
(18) Wang, S.; Liu, B.; Gaylord, B. S.; Bazan, G. C. *Adv. Funct. Mater.* **2003**, *13*, 463−467.
(19) Ho, H. A.; Béra-Abérem, M.; Leclerc, M. *Chem.−Eur. J.* **2005**, *11*, 1718−1724.
(20) McQuade, D. T.; Hegedus, A. H.; Swager, T. M. *J. Am. Chem. Soc.* **2000**, *122*, 12389−12390.
(21) Liu, B.; Gaylord, B. S.; Wang, S.; Bazan, G. C. *J. Am. Chem. Soc.* **2003**, *125*, 6705−6714.
(22) Wang, S.; Bazan, G. C. *Adv. Mater.* **2003**, *15*, 1425−1428.
(23) He, F.; Tang, Y.; Wang, S.; Li, Y.; Zhu, D. *J. Am. Chem. Soc.* **2005**, *127*, 12343−12346.
(24) Xu, Q.-H.; Gaylord, B. S.; Wang, S.; Bazan, G. C.; Moses, D.; Heeger, A. J. *Proc. Natl. Acad. Sci. U.S.A.* **2004**, *101*, 11634−11639.
(25) Bronich, T. K.; Nguyen, H. K.; Eisenberg, A.; Kabanov, A. V. *J. Am. Chem. Soc.* **2000**, *122*, 8339−8342.

DNA, RNA, and proteins.[1,5,8−10,14,17,18,21−23,26−28] Such rigid polymer structures cannot adapt to the range of secondary structures presented by biological macromolecules. Some efforts have been made to increase the conformation freedom of polymers with a range of backbone regiochemistries, with which high sensitive detection are achieved as expected because of the improved contacts with better spatial interaction between polymers and biological macromolecules.[2,11,15−17,19,29] Recently, Ho et al. reported an impressive detection of PCR-free DNA based on the FRET measurements with flexible cationic polythiophene as transducer, where this water-soluble conjugated polymer exhibits color and fluorescence changes when put in the presence of single-stranded or double stranded nucleic acids.[30] Obviously, this is a specific FRET measurement with the great potential for ultrasensensitive detections based on conjugated polymers. Although the strong electrostatic interactions between CCPs and target bioploymers could bring them into very close proximity, the color changes of the flexible polymers are not usually desirable for most of FRET applications upon binding with target species because the optical properties of CCPs and the fluorescence dyes should satisfy the spectral requirements for efficient FRET from donor to acceptor.[11,15,16,19,24,31] Therefore, a flexible CCP without significant color change upon binding to different shape analytes is required for FRET measurement. The interactions between CCPs and biopolymers related to the geometry, size, and negative charges of target biopolymers are not yet well understood spectrally. Recently, Liu et al. reported the optimization of the molecular orbital energy of CCPs for the fluorescent sensors, in which they suggested that the possible photoinduced charge transfer may lead to some fluorescence quenching from CCPs and chromophores and, therefore, causes an energy waste during FRET measurement.[14] Meanwhile, it has also been noticed interestingly that the interaction between rigid CCPs and DNA varies with the number of monomer repeat units of CCPs.[18] Furthermore, the unknown spectral properties of the flexible CCPs when complexed to geometry-specific targets further complicate the analysis of observed FRET behaviors. These unexpected phenomena should be correlated with an occurrence of strong interchain and/or intrachain segment interactions of the flexible CCPs. On a broader level, understanding the geometry-specific DNA-dependent spectral properties of flexible CCPs in detail is of considerable importance for fluorescence- and FRET-based DNA detections, as the optical properties of the flexible CCPs are much sensitive to the conformation changes of target biopolymer.[12,15−17,29]

Recently, a flexible, water-soluble, cationic PPV derivative, poly{(2,5-bis(3-bromotrimethylammoniopropoxy)-phenylene-1,4-divinylene)-*alt*-1,4-(2,5-bis(2-(2-hydroxyethoxy)ethoxy))-phenylenevinylene} (BH−PPV), was synthesized.[32,33] Although much attention has been focused on the well-known potential for use of PPV derivatives as electronic materials, the spectral properties of PPV derivatives and their dynamics and dependence on morphology of PPV derivatives have been under active investigation in the last 10 years, in which the light emission mechanism of flexible CCPs is complicated and not well understood yet.[34−36] Furthermore, the highly positively charged flexible PPV could make it a promising model polymer for understanding the interactions and self-assembly properties of negatively charged biopolymers.[4]

Scheme 1. Molecular Structures of BH-PPV and X2-Bound TAMRA

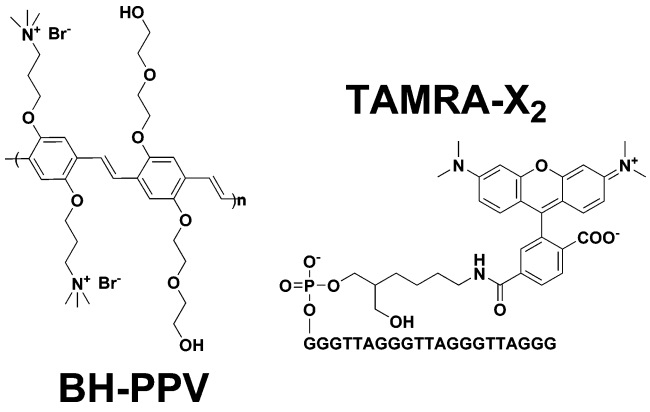

Scheme 1 shows the molecular structures of BH−PPV and ssDNA-bound TAMRA. The resulting polymer is well soluble in aqueous solution, owing to the quaternized amine-terminated groups and hydroxyl (−OH) group attached to the main chain of BH−PPV. The positively charged nature of PPV permits coordination of electrostatic forces with oppositely charged analyte targets, where the flexible backbone would be expected to improve the contacts between optically active groups of PPV and target DNA. Meanwhile, the positive charges at two sides of the backbone of BH−PPV symmetrically could result in the disorder distortion of the flexible CCP backbone upon binding to negatively charged DNA and, therefore, bring many isolated conjugated segments within single polymer. Because of the limited conjugation of isolated segments, there is no obvious change in the spectral position of the BH−PPV that is suitable for FRET application.

Generally, complexation of flexible CCPs with negatively charged biopolymers (such as DNA) may extend or compress the polymer chains related to the geometry, size, and electronic charges of biopolymers and, consequently, leads to changes of the emission of flexible CCPs both in fluorescence intensity and fluorescence peak position.[11,15,16,19] For FRET measurement, it is necessary to find novel analyte shape adaptable flexible CCPs without obvious color changed. In this paper, we report in detail the target conformation-dependent optical properties of the flexible BH−PPV and FRET upon complexation with several kinds of ssDNAs (G-rich ssDNA and DNA hairpin).[37−45]

(26) Pinto, M. R.; Schanze, K. S. *Synthesis-Stuttgart* **2002**, *9*, 1293.
(27) Stork, M. S.; Gaylord, B. S.; Heeger, A. J.; Bazan, G. C. *Adv. Mater.* **2002**, *14*, 361.
(28) Gaylord, B. S.; Massie, M. R.; Feinstein, S. C.; Bazan, G. C. *Proc. Natl. Acad. Sci. U.S.A.* **2005**, *102*, 34−39.
(29) Liu, B.; Wang, S.; Bazan, G. C.; Mikhailovsky, A. *J. Am. Chem. Soc.* **2003**, *125*, 13306−13307.
(30) Ho, H. A.; Doré, K.; Boissinot, M.; Bergeron, M. G.; Tanguay, R. M.; Boudreau, D.; Leclerc, M. *J. Am. Chem. Soc.* **2005**, *127*, 12673−12676.
(31) Lakowicz, J. R. *Principle of Fluorescence Spectroscopy*; Plenum: New York, 1999.
(32) Li, H.; Li, Y.; Zhai, J.; Cui, G.; Liu, H.; Xiao, S.; Liu, Y.; Lu, F.; Jiang, L.; Zhu, D. *Chem.−Eur. J.* **2003**, *9*, 6031−6038.
(33) Jiang, L.; Lu, F.; Chang, Q.; Liu, Y.; Liu, H.; Li, Y.; Xu, W.; Cui, G.; Zhuang, J.; Li, X.; Wang, S.; Song, Y.; Zhu, D. *ChemPhysChem.* **2005**, *6*, 481−486.
(34) Peng, K. Y.; Chen, S. A.; Fann, W. S. *J. Am. Chem. Soc.* **2001**, *123*, 11388−11397.
(35) Nguyen, T.-Q.; Wu, J.; Doan, V.; Schwartz, B. J.; Tolbert, S. H. *Science* **2000**, *288*, 652−656.
(36) Bout, D. A. V.; Yip, W.-T.; Hu, D.; Fu, D.-K.; Swager, T. M.; Barbara, P. F. *Science* **1997**, *277*, 1074−1077.
(37) Ueyama, H.; Takagi, M.; Takenaka, S. *J. Am. Chem. Soc.* **2002**, *124*, 14286−14287.

The fluorescence intensity change of BH−PPV due to the conformation changes of the flexible conjugated backbone can help us to distinguish various DNA with different geometries according to the specific optical properties of the CCPs and the DNA-bound fluorescence dyes. The properties of the changed fluorescence intensity upon binding with specific biopolymers without obvious color changes make BH−PPV a suitable CCP donor to determine the biomolecular structure based on FRET measurements. The results of this study could provide some fundamental understanding of the spectral properties of flexible water-soluble BH−PPV and CCPs/DNA interaction related to sizes and geometry of target analyte, which paves a way to determining the geometry-dependent conformation of biomolecules such as DNA and proteins based on FRET by using flexible CCPs.

Materials and Methods

Materials. PPV derivative poly {(2,5-bis(3-bromotrimethylammoniopropoxy)-phenylene-1,4-divinylene)-*alt*-1,4-(2,5-bis(2-(2-hydroxyethoxy)ethoxy))phenylenevinylene} (BH−PPV) was synthesized as described elsewhere.[32,33] Gel permeation chromatography (GPC) analysis shows that the BH−PPV has an MW of 13 798, Mn of 12 776, and Mz of 15 267, with MW/Mn of 1.08. This polymer has 17 repeat units. The length of BH−PPV is estimated to be about 23.8 nm according to the MM2 method.

Labeled and unlabeled oligonucleotides were purchased from Shanghai Sangon Biological Engineering Technology & Service Co., Ltd. For all FRET measurements, the TAMRA dye was labeled at the 5′-termini of the oligonucleotide as the acceptor. The DNA concentrations were determined by measuring the absorbance at 260 nm in a 250μL quartz cuvette. The buffer contained 5 mM Tris−HCl at pH 7.5. The water was purified using a Millipore filtration system.

General Procedure for Optical Measurements. Absorption spectra were recorded on a UV−vis spectrophotometer (Model U-3010, Shimadzu). Fluorescence spectra were recorded on a Hitachi F-4500 fluorescence spectrophotometer. Fluorescence lifetimes were recorded on a time-correlated single photon counting (TCSPC) spectrophotometer (FLS 920, Edinburgh Analytical Instruments) with IRF about 100 ps. The fluorescence decay curves were fitted with a double-exponential function by FluoFit software (Version 3.1, PicoQuant, Germany). The fitting quality was judged by weighted residuals and reduced χ^2 values.

All experiments were recorded at 25 °C except specific. For all optical measurements, 3 mL quartz cells with an optical path length of 1.0 cm were utilized.

Sequences of the ssDNAs Studied. Three model ssDNAs were used in this work because of their known folding and unfolding properties. They are the G-rich ssDNAs with the sequences as 5′-GGTTGGTGTGGTTGG-3′(X1) and 5′-GGGTTAGGGTTAGGGTTAGGG-3′-(X2),[37−42] as well as DNA hairpin with the sequence as: 5′-CTCTTCAGTCAAAAAAAAAAAAAAAAAAAAGACTGAAGAG-3′.[43−45]

Sample Preparation. (a) G-Quadruplex Folding of G-rich ssDNA. To prepare the complex of ssDNA/BH−PPV, in brief, both 10 μL of ssDNA (1.0×10^{-4} M) and 50 μL of BH−PPV (1.0×10^{-5} M) were added into two 1.5 mL Eppendorf cups, respectively. The samples were treated at 0 °C for 1 h to form stable complexes. Once 50 μL of 1.0 M KCl was added into one Eppendorf cup, the BH−PPV warped G-Quadruplex Folding state of X1 (or X2) was formed, stabilized by K^+ ion.[37−42] Once 50 μL of 5 mM Tris-HCl was added into the other one, the extending rigid rodlike BH−PPV/X1 (or X2) complex was formed.[37−42] The final concentrations of BH−PPV and X1 (or X2) for spectral measurements were 1.0×10^{-7} and 1.0×10^{-6} M, respectively.

(b) Folding and Unfolding of the DNA Hairpin. To prepare the complex of DNA hairpin and BH−PPV, in brief, 10 μL of DNA hairpin (1.0×10^{-4} M) and 940 μL of 5 mM Tris−HCl were added into a 1.5 mL Eppendorf cup, and the sample was kept at 65 °C for 20 min to make the DNA hairpin in open state.[43−45] The rigid rodlike BH−PPV/DNA hairpin complex was formed after adding 50 μL of BH−PPV (1.0×10^{-5} M) at 65 °C. Then the sample was slowly cooled to 25 °C, where the close state was formed.[43−45] The final concentrations BH−PPV and DNA hairpin for spectral measurements were 1.0×10^{-7} and 1.0×10^{-6} M, respectively.

Single Molecule Spectroscopy. Single molecule measurements were performed with a time-resolved confocal fluorescence microscope (MicroTime 200, PicoQuant, Germany), in which single molecule fluorescence images were recorded by raster scanning the sample through the excitation light focus by means of a linearized $x-y-z$ piezo scanner. Samples were prepared for single molecule measurements by spin casting solutions of BH−PPV(1.0×10^{-7} M)/ssDNA (1.0×10^{-6} M) complex and poly(vinyl alcohol) (PVA) as polymer matrix in solution onto a clean glass coverslip. This yields 100−200 nm thick polymer films. Individual molecules were positioned sequentially in the laser focus to measure the fluctuations in fluorescence intensity with time. A PC plug-in card (TimeHarp200, PicoQuant, Berlin, Germany) was used to register the detected photon from single-photon avalanche diodes (SPCM AQR-13, Perkin-Elmer, ~60% quantum yield of detection at 670 nm, less than 150 dark counts per second). The intensity time-trace with 100 ns time resolution on a continuous time axis relative to the start of the measurement could be achieved. For excitation, a pulsed laser diode (442 nm, 100 ps, 40 MHz) (LDH, PicoQuant, Germany) was used. The collimated laser beam after a polarization-maintaining single mode fiber was changed from linear to circular by a polarizer and a λ/4-plate and spectrally filtered by an excitation filter (D440/10, Chroma, USA) before being directed into the inverted microscope body (Olympus IX 71). A dichroic mirror (455DRLP, Omega, USA) reflects the laser light into a high aperture oil immersion objective (100 ×, NA1.4, PlanApo, Olympus). Sample fluorescence is collected through the same objective and transmitted through the dichroic mirror. After passing one emission band-pass filter (FF495, Semrock, US), a tube lens (200 mm focal length) focuses the fluorescence onto a 100 μm pinhole for confocal imaging. The fluorescence after this pinhole was refocused onto the active area of the avalanche diode (SPAD). All single molecule measurements were performed in an N_2 atmosphere allowing for both a better observation of fluorescence and a large increase in the photochemical stability of BH−PPV molecules.

Results and Discussion

Figure 1 shows the absorption and fluorescence spectra of BH−PPV and X2-bound TAMRA. For BH−PPV, the absorbance maximum is centered at about 420 nm, which is attributed to the electron transition of $\pi-\pi^*$ along the conjugated polymer main chain,[33,46] and the emission maximum is centered at 520 nm. The absorbance maximum of X2-bound TAMRA dye is about 560 nm and the emission peak is centered at 590 nm. It is found that there is large spectral overlap between the CCP and fluorescent dye TAMRA, indicating that efficient FRET between the polymer and the dye could be encouraged.

Figure 2 shows the FRET spectra of BH−PPV and TAMRA bound with X1 and X2 in the presence and absence of K^+ ions excited at 420 nm. The relative fluorescence intensities of

(38) Weitamann, M. N.; Woodford, K. J.; Usdin, K. *J. Biol. Chem.* **1996**, *271*, 20958−20964.
(39) Walmsley, J. A.; Burnett, J. F. *Biochemistry* **1999**, *38*, 14063−14068.
(40) Lu, M.; Guo, Q.; Kallenbach, N. R. *Biochemistry* **1992**, *31*, 2455.
(41) Willamon, J. R. *Annu. Rev. Biophys. Biomol. Struct.* **1994**, *23*, 703−730.
(42) Hud, N. V.; Smith, F. W.; Anet, F. A. L.; Feigon, *J. Biochemistry* **1996**, *35*, 15383−15390.
(43) Grunwell, J. R.; Glass, J. L.; Lacoste, T. D.; Deniz, A. A.; Chemla, D. S.; Schultz, P. G. *J. Am. Chem. Soc.* **2001**, *123*, 4295−4303.
(44) Bonnet, G.; Krichevsky, O.; Libchaber, A. *Proc. Natl. Acad. Sci. U.S.A.* **1998**, *95*, 8602−8606.
(45) Syvänen, A.-C. *Nat. Rev. Genet.* **2001**, *2*, 930−942.

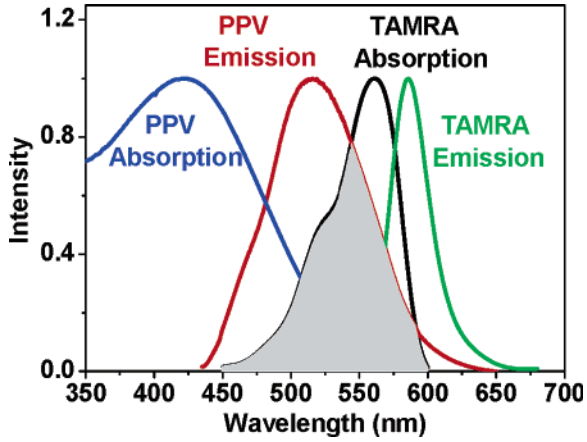

Figure 1. Normalized absorption and fluorescence spectra of BH−PPV and X2-bound TAMRA. The shaded area shows the spectral overlap.

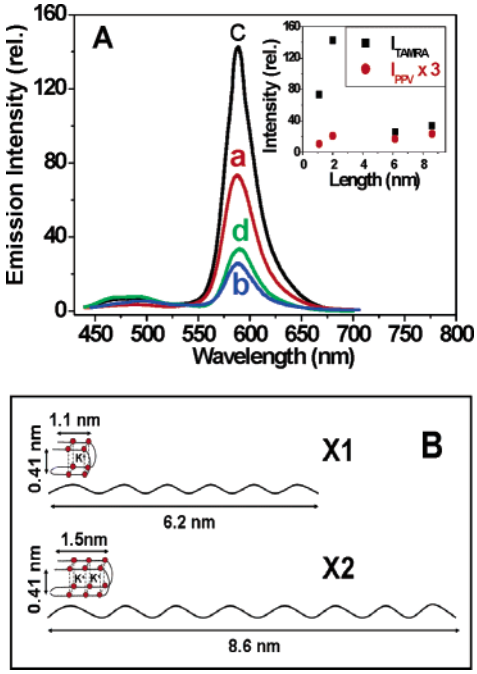

Figure 2. (A) Fluorescence from solutions containing BH−PPV and (a) X1-TAMRA in the presence of K^+ ion; (b) X1-TAMRA in the absence of K^+ ion; (c) X2- TAMRA in the presence of K^+ ion and (d) X2- TAMRA in the absence of K^+ ion. [X1-TAMRA] or [X2-TAMRA] = 1.0×10^{-6} M, and [BH−PPV] = 1.0×10^{-7} M. The inset shows the relative fluorescence intensity of TAMRA (and BH−PPV) vs persistence length of G-rich ssDNA (X1 and X2) at different folding states with or without K^+ ions. The fluorescence intensity of BH−PPV was enlarged by 3 times for BH−PPV in the inset. The excitation wavelength was 420 nm. (B) Schematic representation of the persistence lengths of G-quadruplex X1 and X2 in the presence of K^+ ion, as well as random coil X1 and X2 in the absence of K^+ ion.

TAMRA upon estimated persistence lengths of X1 and X2 at various folded (in the presence of somewhat of K^+ ions) and unfolded (in the absence of K^+ ions) states are also shown in the inset of Figure 2. Excitation at 420 nm selectively excites the BH−PPV, and the fluorescence from TAMRA thus results from the excited BH−PPV by FRET. Surprisingly, we found that the fluorescence intensities of TAMRA transferred from excited BH−PPV are obviously different with different DNA geometries. As control experiments, we did not find the obvious changes of fluorescence spectra (intensity and peak position) of TAMRA upon direct excitation of the TAMRA at 530 nm when TAMRA was attached to ssDNA, indicating that there is no significant quenching of TAMRA upon interaction with various ssDNAs mentioned in ref 14. The FRET-dependent TAMRA fluorescence intensity thus strongly depends on the ssDNA conformations. The FRET between BH−PPV and TAMRA is effective when X1 (or X2) is folded in the presence of K^+ ions, and becomes less effective in the absence of K^+ ions (as shown in Figure 2) or upon adding complementary chains of X1 and X2 into folded X1 (or X2) in the presence of K^+ ion (data not shown). We believe that the unexpected fluorescence and FRET behaviors in these cases could result from different BH−PPV conformations modulated by DNA geometry. These unexpected phenomena are expected to be correlated with an occurrence of strong interchain and/or intrachain interactions of the BH−PPV, where the interactions including excimers (or exciplexes) and aggregates within single polymer chain and/or ensemble polymers lead to the observed changes in fluorescence spectra similar to most flexible polymers.[15,16,34] Furthermore, unlike those rigid polymers with long conjugated segments,[1,5,8−10,14,17,18,21−23,26,27] flexible PPV is not the long-chain limited case; many defects formed during synthesis interrupts the polymer main chains,[34,46,47] leading to many limited conjugated chain units (segments) in PPV polymers.[48−51] Furthermore, the cationic charges are located at the two sides of BH−PPV backbone symmetrically; the distortion (bending and twisting) of the polymer backbone can be randomly induced by high charge density ssDNA(G-rich) through the electrostatic interaction, which further produces more isolated conjugated segments within single polymer. The interaction among these different segments within BH−PPV chains could be modulated with different DNA geometries; the observed fluorescence of BH−PPV is therefore a superposition of all the interacted segments in PPV. Hence, the broad structureless fluorescence spectra of PPV have the contributions from both of isolated segments and aggregated intrachain segments. To prove this assumption, a detail understanding of the DNA geometry dependent spectral properties of flexible BH−PPV is then required.

To determine these spectral characteristics of BH−PPV upon binding with different geometric ssDNAs, we measure the ensemble fluorescence spectra of BH−PPV in the presence of TAMRA-free ssDNA (G-rich X1 and X2). To avoid the aggregation of DNA and BH−PPV at high concentration caused by hydrophobic interactions, all the experiments were carried out at very low concentration around 10^{-6} M for DNA and 10^{-7} M for BH−PPV in solution, where the electrostatic interaction dominates at low concentration.[24] Thus, the fluorescence can be taken from single polymer in dilute solution, where the aggregation (interchain interaction) is not considered necessary for the observed spectral changes upon BH−PPV binding to ssDNA. For the sake of comparison, the concentration of BH−PPV or DNA for all measurements was kept the same, where 1:10 complex ratio between BH−PPV and DNA was used to

(46) Chen, Z. K.; Meng, H.; Lai, Y. H.; Huang, W. *Macromolecules* **1999**, *32*, 4351−4358.
(47) Padmanaban, G.; Ramakrishnan, S. *J. Am. Chem. Soc.* **2000**, *122*, 2244−2251.
(48) Gettinger, C. L.; Heeger, A. J. *J. Chem. Phys.* **1994**, *101*, 1673−1678.
(49) Hsu, J.-H.; Fann, W. *J. Phys. Chem. A* **1999**, *103*, 2375−2380.
(50) Woo, H. S.; Lhost, O.; Graham, S. C.; Bradley, D. D. C.; Friend, R. H.; Quattrocchi, C.; Brédas, J. L.; Schenk, R.; Müllen, K. *Synth. Met.* **1993**, *59*, 13−28.
(51) Hu, D.; Yu, J.; Barbara, P. F. *J. Am. Chem. Soc.* **1999**, *121*, 6936−6937.

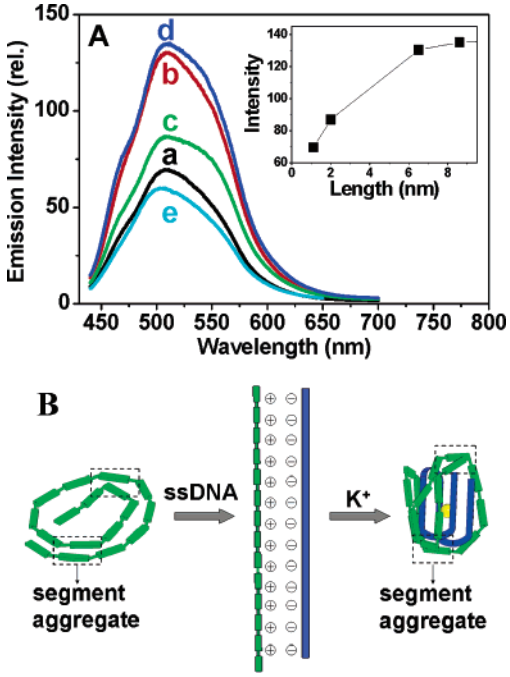

Figure 3. (A) Fluorescence from solutions containing BH−PPV and (a) X1 in the presence of K^+ ion; (b) X1 in the absence of K^+ ion; (c) X2 in the presence of K^+ ion and (d)X2 in the absence of K^+ ion. (e) Fluorescence from free BH−PPV in solution without binding ssDNA is also shown for comparison, where the free BH−PPV in solution with low fluorescence intensity seems to adapt more compact aggregate because of the good solubility and flexibility. [X1] or [X2] = 1.0×10^{-6} M, and [BH−PPV] = 1.0×10^{-7} M. The inset shows the relative fluorescence intensity of BH−PPV vs persistence length of G-rich ssDNA (X1 and X2) at different folding states with or without K^+ ions. The excitation wavelength was 420 nm. (B) Major interactions within BH−PPV/X1 complexes at different states that influence the optical performance of BH−PPV. The formation of BH−PPV/X2 complexes is similar to that of BH−PPV/X1 complex.

ensure that each BH−PPV was bound to ssDNA during measurements.

Figure 3 shows the DNA geometry dependent fluorescence spectra of BH−PPV. We found that the fluorescence intensity of BH−PPV increases with the persistent lengths of negative charged ssDNAs (see inset in Figure 3). In fact, in the presence of ssDNA (G-Rich) without adding K^+ ion, a stoichiometric complex between unfolded anionic ssDNA and the BH−PPV tends to be insoluble in the solution in which a rodlike complex is formed.[15−17] In this case, the BH−PPV chains are extended. Previous study indicated that there were unavoidable defects during synthesis that lead to many limited conjugated segments within single PPV.[52] Considering the fact that the absorption and emission transition dipole moments of isolated segments in extended conjugated polymers are oriented along the polymer chain, together with the presence of unavoidable defects during polymer synthesis, dipoles from segments along a chain are poorly situated for efficient Förster transfer; the intrachain energy migration among isolated segments cannot occur efficiently via Förster transfer. Therefore, the fluorescence of BH−PPV with extended conformation exhibits strong emission, contributed from multiple emitting segments. The enhanced fluorescence from BH−PPV is a superposition of all the segments in single BH−PPV. Upon adding K^+ ion, the formation of folded G-quadruplex state of X1 (or X2) stabilized by K^+ ion has a much higher space charge density, which allows flexible BH−PPV to wrap tightly around the folded G-quadruplex structure through electrostatic interactions.[15,23] This will bring the segments closer together and lead to intrachain segment aggregates in BH−PPV. Unlike the extended BH−PPV in which there is no favorable energy transfer, the wrapped BH−PPV around folded ssDNA leads to the parallel face-to-face transition dipole moments among the intrachain segments, resulting in classical excimer/exciplex-type behavior. In addition to the intrachain segment aggregation mentioned above, the folded ssDNA(G-Rich) binding with the polymer produces a tightly wrapped complex, forcing the polymer backbone to be more distorted. Importantly, because the cationic charges are symmetrically located at the two sides of BH−PPV backbone, side-chain disordering of the flexible BH−PPV can be randomly induced by high charge density ssDNA(G-rich) through the electrostatic interaction, leading to further distortion (twisting) of the polymer chain. Any bending or twisting of the flexible PPV backbone will result in breaks in the π-conjugation and bring more isolated conjugation segments within single polymer. The distortion of the BH−PPV further reduces the observed fluorescence intensity. The reduction of the BH−PPV fluorescence intensity is due not only to the formation of intrachain segment aggregations, but also to single polymer chain distortion (steric hindrance and phenylenevinylene unit twisting around the folded G-rich ssDNA), resulting in the serious π-conjugation interruption. As shown in Figure 3B, the persistent length of the smallest folded X1 (G-rich) is about 1.1 nm, and the increased charged density of folded DNA brings about tight wrapping of the flexible BH−PPV around the folded DNA surface. The flexible BH−PPV with 23.8 nm chain length can wrap the folded X1(G-rich) in two or three cycles, which tends to distort the backbone and/or form more isolated segment aggregates. Therefore, the delocalization of π-elecetrons is thought to be limited by folding induced distortion of backbone and chemical defects on the chain, leading to formation of isolated segment units. Basically, there are two types of chromophores within a flexible BH−PPV upon binding with ssDNA; we refer to these two as the "isolated" segment and the "packed" segment aggregates. The fluorescence intensity of the aggregated segments is dramatically reduced relative to that of isolated segments. The smaller the size of DNA is, the stronger the segment interactions are, whereas the weaker the fluorescence intensity is.

Table 1. Fitting Parameters of Fluorescence Lifetimes of BH−PPV/X1 (and X2) Complexes at Different Conditions

BH–PPV/DNA complex	lifetime			
	τ_1 (ns)	amplitude (%)	τ_2(ns)	amplitude (%)
X1 with K^+	0.412	55	1.575	45
X1 without K^+	0.55	61	1.725	39
X2 with K^+	0.645	60	1.815	40
X2 without K^+	0.655	63	1.848	37

Fluorescence lifetime measurements further prove the formation of intrachain segment aggregations. In addition to the intensity changes, the time-resolved fluorescence lifetime measurement shows the corresponding change in the decay dynamics with two decay components. Table 1 lists the fluorescence lifetimes of BH−PPV/X1 (and X2) complexes at different conditions. The shorter lifetime is from the isolated segments, which contributed the observed fluorescence, whereas

(52) Hu, D.; Yu, J.; Wong, K.; Bagchi, B.; Rossky, P. J.; Barbara, P. F. *Nature* **2000**, *405*, 1030−1033.

the longer lifetime is from the aggregated segments, which caused the fluorescence quenching because of the formation of nonfluorescent excimers/exciplexes among segments. Considering the fact that there is little change in the spectral shift, the long-lived fluorescence decay may be associated with the singlet state following back transfer from the nonemissive intrachain segment aggregate to the excited state of isolated segments. The amplitude ratio between the two delay components depends on the size of the folded and unfolded ssDNAs (G-rich). In the presence of folded X1 as shown in Table 1, the increasing amplitude of the long decay component indicates the formation of the high-density intrachain segment aggregates within BH−PPV when wrapped tightly around the folded ssDNA stabilized by K^+ ion.[53,54]

To further determine the formation of the isolated segments and intrachain segment aggregates, we perform the single molecule measurements of single BH−PPV/X1 complex in the presence and absence of K^+ ions. Figure 4 shows the typical fluorescence intensity time traces of BH−PPV/X1 complexes in the presence of K^+ ions in solution. Three kinds of the time traces are found: trace (a) shows an example of a single BH−PPV molecule emitting photons with rapid intensity switches between on and off and shows typical single molecule behavior with one-step photobleaching, whereas trace (b) shows an example of stepwise photobleaching, and trace (c) shows the fluorescence from a single BH−PPV molecule with nearly constant count rate without photobleaching during observation time. The one-step photobleaching as shown in trace (a) is typically from single isolated segments or from very few isolated segments, whereas the stepwise photobleaching in trace (b) and nonphotobleaching in trace (c) are from multi-isolated segments within single BH−PPV. Figure 4B shows the normalized histograms of the trace (a), trace (b), and trace (c) of BH−PPV/X1 in the presence and absence of K^+ ions. Compared to the BH−PPV/X1 complex in the absence of K^+ ion, more BH−PPV shows the single molecule behaviors as shown in trace (a) of Figure 4, indicating less isolated segments and more nonfluorescence segment aggregates are formed in folded X1. Figure 4C shows the normalized histograms of the surviving time distributions for those single BH−PPV molecules with similar behavior of stepwise photobleaching to trace (b); the surviving times of BH−PPV/X1 complex in the presence of K^+ ion is also shorter, indicating that less isolated segments of BH−PPV/folded X1 complex is formed compared with that of BH−PPV/unfolded X1 complex. Single molecule measurements further demonstrate that there are less isolated segments and more nonfluorescence segment aggregates are formed when BH−PPV was complexed with folded X1 compared to that with unfolded X1.

Generally, it is known that there is a strong correlation between the spectral properties and the backbone conformations of CCPs. The reduction of the fluorescence of BH−PPV in folded X1 (or X2) is finally from the diminishing number of light-emitting excitons because of the flexible backbone distortions and intrachain segment aggregates. Fortunately, because of the existence of abundant isolated conjugation segments, except from the obvious changes in the fluorescence intensity

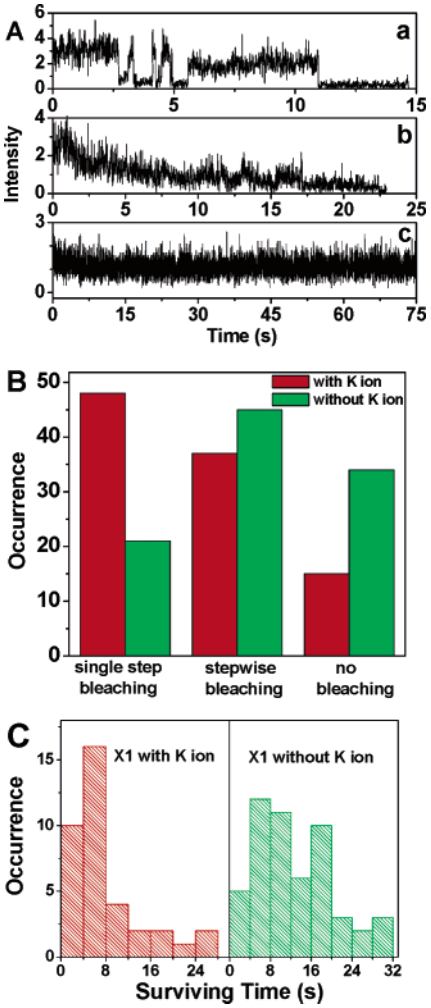

Figure 4. (A) Three typical fluorescence intensity time traces of single BH−PPV/X1 complex in the presence of K^+ ions in solution with an integration time of 1 ms/bin at an excitation intensity of about 1.5 kW/cm^2. (a) single molecule behavior; (b) stepwise photobleaching; and (c) no photobleaching. (B) Histograms of these three typical fluorescence intensity-time traces of single BH−PPV/X1 complex in the presence and absence of K^+ ions in solution. (C) Surviving times histograms for those stepwise single BH−PPV/X1 complex with and without K^+ ions in solution.

as shown in Figure 3, the spectra of BH−PPV in all the cases are almost identical without significant wavelength shift, indicating that the conformation of BH−PPV is in a rather disordered state and therefore a limited conjugate for BH−PPV upon binding with ssDNA. The fluorescence intensity of isolated segments is higher than that of aggregation. The intrachain segment aggregates within single BH−PPV chain in solution lead to quenching of excitons by formation of nonemissive excited states and, therefore, reduce the emission intensity. The less spectral shift of BH−PPV with a large change of fluorescence intensity makes flexible BH−PPV a suitable donor for the FRET measurements to determine the geometry-specific folding and unfolding conformations of DNA. With this advantage for flexible CCPs such as BH−PPV used here, this could pave an alternative way to determining the geometry-dependent conformation changes of biomolecules such as DNA and proteins based on FRET by means of flexible CCPs.

As a typical example, the structure of DNA hairpin could be detected by flexible BH−PPV based on the FRET measurements. DNA hairpins are inverse repeats of single-stranded DNA

(53) Klärner, G.; Former, C.; Yan, X.; Richert, R.; Müllen, K. *Adv. Mater.* **1996**, *8*, 932−935.
(54) Egelhaaf, H.-J.; Gierschner, J.; Oelkrug, D. *Synth. Met.* **1996**, *83*, 221−226.

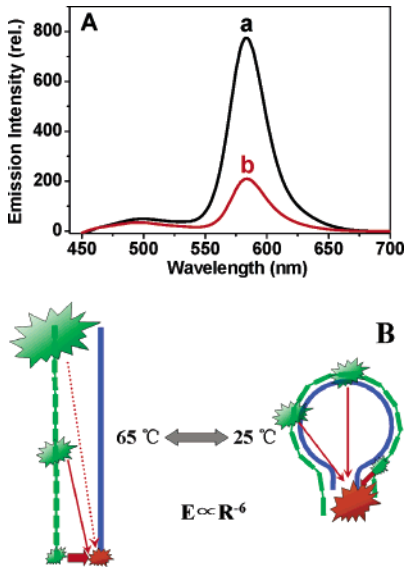

Figure 5. (A) Relative fluorescence from solutions containing the BH−PPV/DNA hairpin complexes at 25 °C (a) and 65 °C (b). [DNA hairpin] = 1.0×10^{-6} M, and [BH−PPV] = 1.0×10^{-7} M. Excitation wavelength was 420 nm. (B) Principle of the specific detection of the conformations of DNA hairpin at its "open" and "close" states.

connected by a noncomplementary loop sequence, and they are one of the simplest structures that a nucleic acid polymer can form.[43,44] To demonstrate this specific detection, a well-studied DNA hairpin with the sequence as 5′-CTCTTCAGTCAA-AAAAAAAAAAAAAAAAAAGACTGAAGAG-3′, was used here for FRET measurement,[43−45] where TAMRA was labeled at 5′-temini as acceptor. There are 10 bases in the stem of the DNA hairpin, and the DNA hairpins are in the closed state when the complementary bases of the stem form intramolecular hydrogen bonds and present a secondary structure with one helix.[43] The open and closed states of this DNA hairpin are reversible and can be modulated easily by simply changing the temperature of solution as described in refs 43 and 44. The persistence lengths of DNA hairpin at its open and closed states are estimated about 16 nm. The loop part in its closed state is still free, and very little length changed along the loop.

During FRET measurement, the 1:10 complex ratio between BH−PPV and DNA hairpin was mixed into buffer to ensure every BH−PPV in solution can be complexed to DNA hairpin. Figure 5 shows the FRET measurement between BH−PPV and TAMRA-attached DNA hairpin upon excitation at 420 nm. When BH−PPV is bound electrostatically to "open" DNA hairpin at 65 °C, they form an insoluble rodlike structure in solution.[16,23] Although each isolated segment in BH−PPV acts as a donor, the segments line up along the extended polymer chain one by one far away from the TAMRA dye that attached to the end of ssDNA hairpin; only a few segments close to the acceptor TAMRA can transfer their energy to acceptor TAMRA; because of the requirement of R_{DA}^{-6},[31] the FRET is inefficient. When the temperature falls down to 25 °C, the DNA hairpins turn to a "closed" state, and the flexible BH−PPV was wrapped electrostatically and extended along the DNA hairpin loop in a rigid form; every isolated segments in BH−PPV are approached to close to the terminal TAMRA dye; FRET efficiency was thus obviously enhanced. We thus observe strong TAMRA fluorescence transferred from every segment of BH−PPV. The scheme of the specific detection is shown in Figure 5. Because the detection is performed at low concentration of BH−PPV, single molecule sensitivity could be achieved. Such kind of energy transfer is very similar to that which occurs within phycobilisomes, a light-harvesting pigment-array in the photosynthetic cyanobacterial cell, where the sunlight is captured from the peripheral pigment-array and transferred efficiently to the central terminal trap.[55,56]

Conclusion

In conclusion, we report the detection of analyte shape-specific DNA structure with a novel flexible CCP based on the FRET. Complexation with negatively charged DNA modulates the optical properties of flexible CCP, which is responsive to the analyte shape. The conformation-dependent spectral properties of BH−PPV are investigated by means of ensemble and single molecule measurements, which can interpret the observed unexpected FRET phenomena. Both the fluorescence and fluorescence lifetime measurements verify the coexistence of isolated segments and intrachain segment aggregates as multichromophore molecules within a single BH−PPV chain. We found that the fluorescence spectral shapes and positions of BH−PPV have no significant changes in all cases, where the folded and unfolded DNA controls the number of emitting segments, and therefore control the fluorescence intensity of PPV. The change in fluorescence intensity upon binding with shape-specific DNA without obvious spectral shift makes this novel flexible polymer a suitable CCP donor to determine the biomolecular structure based on FRET measurements. This study paves a way to designing suitable processing protocols by using flexible CCPs for the identification of the analyte geometries, especially the geometry-dependent interaction between DNA and a protein, such as aptamer and human α-thrombin interaction.[15,16,19]

Acknowledgment. We thank Prof. Shu Wang for valuable suggestions and discussion. This work was financially supported by NSFC (90306013 and 30270338), State Key Project for Fundamental Research (2003CB716900), National Center for Nanoscience and Technology of China, and Key Laboratory of Photochemistry of Institute of Chemistry, CAS.

JA063004Y

(55) MacColl, R. J. *Struct. Biol.* **1998**, *124*, 311−334.
(56) Glazer, A. N.; Yeh, S. W.; Webb, S. P.; Clark, J. H. *Science* **1985**, *227*, 419−423.